Inorg. Chem. **1989**, *28*, 1349–1357

Contribution from the Department of Chemistry, University of Manchester Institute of Science and Technology,
PO Box 88, Manchester M60 1QD, United Kingdom, Department of Chemistry, Gorlaeus Laboratories, Leiden University,
PO Box 9502, 2300 RA Leiden, The Netherlands, Laboratory of Chemical Physics, Chemische Laboratoria
der Rijksuniversiteit, University of Groningen, Nijenborgh 16, 9747 AG Groningen, The Netherlands,
and Department of Chemistry, State University of New York at Albany, Albany, New York 12222

X-ray Absorption Edge Spectroscopy of Copper(I) Complexes. Coordination Geometry of Copper(I) in the Reduced Forms of Copper Proteins and Their Derivatives with Carbon Monoxide

Ninian J. Blackburn,*[1a,b] Richard W. Strange,[1a] Jan Reedijk,[1c] Anne Volbeda,[1d] Amjad Farooq,[1e]
Kenneth D. Karlin,[1e] and Jon Zubieta[1e]

Received July 22, 1988

X-ray absorption edges have been measured for a variety of Cu(I) complexes of known structure. The structures of these complexes vary in a systematic way from linear two-coordinate through distorted trigonal and trigonal-pyramidal to tetrahedral stereochemistry. The structure of one of the model complexes, $[Cu_2(N3OR)](PF_6)_2{\cdot}CH_2Cl_2$ (**3**-$(PF_6)_2{\cdot}CH_2Cl_2$), is described. **3**-$(PF_6)_2{\cdot}CH_2Cl_2$, $C_{45}H_{48}Cl_2Cu_2F_{12}N_6O_2P_2$, crystallizes in the triclinic space group $P\bar{1}$ with $Z = 2$ and $a = 12.430$ (4) Å, $b = 13.456$ (3) Å, $c = 15.497$ (4) Å, $\alpha = 81.75$ (2)°, $\beta = 83.43$ (2)°, and $\gamma = 79.68$ (2)°. The structure consists of one discreet complex dication and two well-separated anions per asymmetric unit. The two crystallographically independent cuprous ions are each three-coordinate with ligation from two pyridine and one tertiary amino donor groups. The Cu–N(py) distances ($\text{Cu–N(py)}_{\text{av}}$ = 1.90 Å) are among the shortest observed within the tripodal tridentate PY2 group of ligands. The intensity of the 8983-eV absorption edge feature in the X-ray absorption spectra of these complexes is shown to correlate with the degree of distortion of the copper center from the N_3 plane, and a qualitative ligand field analysis is presented that invokes mixing of 4s and $4p_z$ orbitals in the final state wave function. The data indicate that absorption edge spectroscopy is a useful technique for the detection of ligand binding to Cu(I) in protein and enzyme systems and, in favorable circumstances, for indicating the probable coordination geometry. The absorption edges of the reduced forms of superoxide dismutase (SOD), dopamine β-hydroxylase (DBH), and deoxyhemocyanin (deoxy-Hc) have been investigated. The absorption edges of reduced SOD and DBH are consistent with three-coordinate Cu(I) centers with only minor distortions from planarity. The edge of deoxy-Hc on the other hand is more consistent with distorted trigonal or tetrahedral geometry. Comparison with the model compounds suggests that a fourth ligand per copper may be present in deoxy-Hc, additional to the three protein-derived histidine ligands, although the data are also consistent with highly distorted trigonal geometry. On binding of CO, the edge profiles indicate a change toward tetrahedral geometry at one or both coppers, and a model for CO binding is presented. DBH is also shown to bind CO.

There is considerable interest at the present time in the structure and mechanism of copper proteins that bind and or activate dioxygen toward catalytic oxygenation reactions.[2-5] Of particular interest are the monooxygenases, tyrosinase,[4] which catalyzes monophenol hydroxylation, dopamine β-hydroxylase (DBH),[5] which catalyzes benzylic hydroxylation of ring-substituted phenethylamines and related substrates, and the copper-dependent phenylalanine hydroxylase from *Chromobacterium violaceum*.[6] Spectroscopic comparisons[7] and sequence homologies[8] have led to the identification of a dinuclear dioxygen binding site (formulated as $Cu_2^{2+}{-}O_2^{2-}$) in tyrosinase, analogous to that found in the oxygen carrier hemocyanin (Hc).[7a,b] In contrast, no evidence exists for dinuclear copper at the active site of DBH,[5,9] although two coppers per subunit have been implicated in the mechanism[10] with an enzyme-bound hydroperoxide entity proposed as an intermediate.[11] Yet another configuration of prosthetic groups is found in the phenylalanine hydroxylase, which requires a tetrahydropterin cofactor, and contains 1 mol equiv of tightly bound copper, which must be in the Cu(I) form for catalytic activity.[6] A rich and varied chemistry thus exists for copper-catalyzed monooxygenation reactions.

The importance of the Cu(I) centers in these enzymes as the site of dioxygen reactivity has stimulated the successful biomimetic modeling of O_2 binding[12-14] and hydroxylation,[15] culminating in

---

(1) (a) University of Manchester Institute of Science and Technology. (b) Current address: Department of Chemical and Biological Sciences, Oregon Graduate Center, 19600 NW Von Neumann Drive, Beaverton, OR 97006. (c) Leiden University. (d) University of Groningen. (e) State University of New York at Albany.

(2) (a) Malkin, R.; Malmstrom, B. G. *Adv. Enzymol. Relat. Areas Mol. Biol.* **1977**, *33*, 177–244. (b) Solomon, E. I. In *Metal Ions in Biology*; Spiro, T. G., Ed.; Wiley Interscience: New York, 1981; Vol. 3, pp 41–108. (c) Solomon, E. I.; Penfield, K. W.; Wilcox, D. E. *Struct. Bonding* (*Berlin*) **1983**, *53*, 1–57.

(3) (a) Karlin, K. D.; Gultneh, Y. *J. Chem. Educ.* **1985**, *62*, 983–990. (b) Karlin, K. D.; Gultneh, Y. *Prog. Inorg. Chem.* **1987**, *35*, 219–327. (c) Karlin, K. D., Zubieta, J., Eds. *Biological and Inorganic Copper Chemistry*; Adenine: Guilderland, NY, 1986; Vols. 1 and 2.

(4) (a) Lerch, K. *Met. Ions Biol. Systm.* **1981**, *13*, 143–186. (b) Robb, D. A. In *Copper Proteins and Copper Enzymes*; Lontie, R., Ed.; CRC Press: Boca Raton, FL, 1984; Vol. 2, pp 207–241.

(5) (a) Villafranca, J. J. In *Metal Ions in Biology*; Spiro, T. G., Ed.; Wiley Interscience: New York, 1981; Vol. 3, pp 263–289. (b) Ljones, T.; Skotland, T. In *Copper Proteins and Copper Enzymes*; Lontie, R., Ed.; CRC Press: Boca Raton, FL, 1984; Vol. 2, pp 131–57. (c) Stewart, L. C.; Klinman, J. P. *Ann. Rev. Biochem.* **1988**, *57*, 551–592.

(6) (a) Pember, S. O.; Villafranca, J. J.; Benkovic, S. J. *Biochemistry* **1986**, *25*, 6611–19. (b) Pember, S. O.; Benkovic, S. J.; Villafranca, J. J.; Pasenkiewicz-Gierula, M.; Antholine, W. E. *Biochemistry* **1987**, *26*, 4477–83. (c) McCracken, J.; Pember, S.; Benkovic, S. J.; Villafranca, J. J.; Miller, R. J.; Peisach, J. *J. Am. Chem. Soc.* **1988**, *110*, 1069–1074.

(7) (a) Himmelwright, R. S.; Eickman, N. C.; Solomon, E. I. *J. Am. Chem. Soc.* **1979**, *101*, 1576–1586. (b) Himmelwright, R. S.; Eickman, N. C.; LuBien, C. D.; Solomon, E. I. *J. Am. Chem. Soc.* **1980**, *102*, 5378–5388. (c) Himmelwright, R. S.; Eickman, N. C.; LuBien, C. D.; Lerch, K.; Solomon, E. I. *J. Am. Chem. Soc.* **1980**, *102*, 5378.

(8) Lerch, K.; Huber, M.; Schneider, H. J.; Drexel, R.; Bernt, L. *J. Inorg. Biochem.* **1986**, *26*, 213–17.

(9) (a) Blackburn, N. J.; Concannon, M.; Khosrow Shahiyan, S.; Mabbs, F. E.; Collison, D. *Biochemistry* **1988**, *27*, 6001–6008. (b) Blackburn, N. J.; Collison, D.; Sutton, J.; Mabbs, F. E. *Biochem. J.* **1984**, *220*, 447–454. (c) Skotland, T.; Peterssen, L.; Backstrom, D.; Ljones, T.; Flatmark, T.; Ehrenberg, A. *Eur. J. Biochem.* **1980**, *105*, 5–11. (d) Walker, O. A.; Kon, H.; Lovenberg, W. *Biochim. Biophys. Acta* **1977**, *482*, 309–322.

(10) (a) Ash, D. E.; Papadopoulos, N. J.; Colombo, G.; Villafranca, J. J. *J. Biol. Chem.* **1984**, *259*, 3395–3398. (b) Klinman, J. P.; Krueger, M.; Brenner, M.; Edmondson, D. E. *J. Biol. Chem.* **1984**, *259*, 3399–3402. (c) Colombo, G.; Rajashekar, B.; Giedroc, D. P.; Villafranca, J. J. *Biochemistry* **1984**, *23*, 3590–3598.

(11) Miller, S. M.; Klinman, J. P. *Biochemistry* **1985**, *24*, 2114–2127.

(12) (a) Karlin, K. D.; Cruse, R. W.; Gultneh, Y.; Farooq, A.; Hayes, J. C.; Zubieta, J. *J. Am. Chem. Soc.* **1987**, *109*, 2668–2679. (b) Blackburn, N. J.; Strange, R. W.; Cruse, R. W.; Karlin, K. D. *J. Am. Chem. Soc.* **1987**, *109*, 1235–1237. (c) Pate, J. E.; Cruse, R. W.; Karlin, K. D.; Solomon, E. I. *J. Am. Chem. Soc.* **1987**, *109*, 2624–2630. (d) Karlin, K. D.; Ghosh, P.; Cruse, R. W.; Farooq, A.; Gultneh, Y.; Jacobson, R. R.; Blackburn, N. J.; Strange, R. W.; Zubieta, J. *J. Am. Chem. Soc.* **1988**, *110*, 6769–6780.

(13) (a) Karlin, K. D.; Haka, M. S.; Cruse, R. W.; Meyer, G. J.; Farooq, A.; Gultneh, Y.; Hayes, J. C.; Zubieta, J. C. *J. Am. Chem. Soc.* **1988**, *110*, 1196–1207. (b) Blackburn, N. J.; Strange, R. W.; Farooq, A.; Haka, M. S.; Karlin, K. D. *J. Am. Chem. Soc.* **1988**, *110*, 4263–4272.

(14) (a) Thompson, J. S. *J. Am. Chem. Soc.* **1984**, *106*, 8308–8309. (b) Thompson, J. S. *J. Am. Chem. Soc.* **1984**, *106*, 4057–4059.

0020-1669/89/1328-1349$01.50/0

the recent description of the first crystal structure of a copper dioxygen complex.[16] These studies, in parallel with the emerging crystallographic details of the oxygen binding site in deoxyhemocyanin[17] are providing new insights into the biochemistry of Cu(I)–O_2 interactions. However, crystallographic data on the monooxygenase enzymes are still unavailable. Therefore, as part of our continuing studies on this class of copper proteins, we have been involved in the development of spectroscopic probes that will allow investigation of the Cu(I) centers of the reduced enzymes and their interactions with O_2 and substrates.

X-ray absorption spectroscopy (XAS) has emerged as a powerful technique in the study of metalloprotein structure[18] and is unique in being able to observe the local environment of the Cu(I) centers, which are transparent to the majority of other metal-directed spectroscopic probes. Most information has been derived from the analysis of the extended fine structure or EXAFS, which in general produces a radial rather than angular description of the active site structure, although some angular information on, for example, histidine orientation can be extracted by using the multiple scattering formalism.[19,20] Geometrical information is in principle available from a detailed analysis of the fine structure, which is often present on the absorption edge or XANES region of the spectrum. Some success has been achieved in theoretical simulation of the XANES using either a full multiple scattering approach[21] or a scattered wave Xα formalism,[22] which treats the edge structure as arising from the combination of low-energy transitions from an initial 1s core state to a bound molecular orbital and higher energy transitions to continuum states. With the latter approach, assignment and theoretical simulation of the absorption edge spectral features have been greatly facilitated by analyzing the single-crystal polarized XANES of a number of high-symmetry systems of known structure, including pseudotetrahedral $[MoS_2O_2{}^{2-}]$[23] and square-planar Cu(II) complexes.[22] For proteins, however, the opportunity to study the orientational dependence of the absorption edge features via the use of single crystals has been possible for a very limited number of systems such as myoglobin[24] and oxidized plastocyanin,[25] where the structure and orientation of the metal site relative to the crystal axes is already known in detail from crystallography.

Chart I

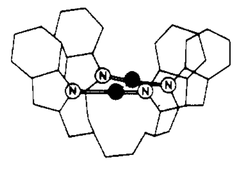

1 $Cu^{I}_2(EDTB)^{2+}$

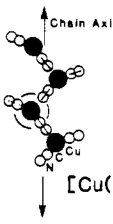

2 $[Cu(CN)_2]^-$

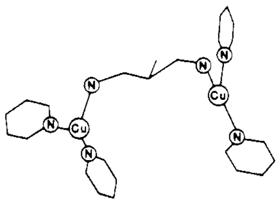

3 $[Cu_2(N3OR)]^{2+}$
$R=(C_6H_5)(C_6H_4)CO_2-$

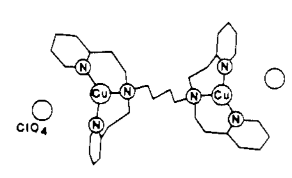

4 $[Cu_2(N4PY2)]^{2+}$

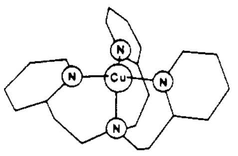

5 $[Cu(TEPA)]^+$

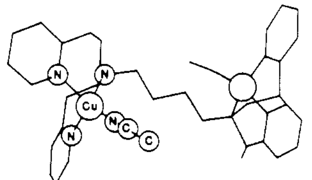

6 $[Cu_2(N4PY2)CH_3CN]^{2+}$

Chart II

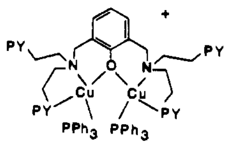

7

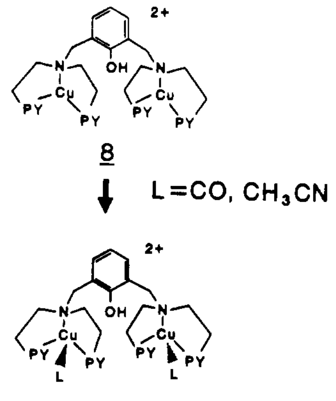

9, L=CO
10, L=CH_3CN

Whichever method is employed, the simulation of XANES is extremely complex and computationally time-consuming. Empirical approaches to the correlation of XANES features with coordination geometry for noncrystalline samples are thus attractive. Kau et al.[26] have recently developed an empirical analysis of edge structure of unoriented systems and convincingly demonstrated the sensitivity of edge structure to coordination environment in a large number of Cu(II) and Cu(I) complexes of known structure. On the basis of quantitative difference edge spectroscopy and a semiempirical ligand field analysis, the two copper atoms of the dinuclear type III site in T2D laccase have been shown to be either both three-coordinate or two- plus four-coordinate. In the present paper we have used a similar approach to investigate the coordination of Cu(I) in the reduced forms of bovine Cu/Zn superoxide dismutase (SOD) and DBH

---

(15) (a) Karlin, K. D.; Hayes, J. C.; Gultneh, Y.; Cruse, R. W.; McKown, J.; Hutchinson, J. P.; Zubieta, J. *J. Am. Chem. Soc.* **1984**, *106*, 2121–2128. (b) Karlin, K. D.; Cohen, B. I.; Jacobson, R. R.; Zubieta, J. *J. Am. Chem. Soc.* **1987**, *109*, 6194–6196.

(16) Jacobson, R. R.; Tyeklar, Z.; Farooq, A.; Karlin, K. D.; Liu, S.; Zubieta, J. *J. Am. Chem. Soc.* **1988**, *110*, 3690–3692.

(17) (a) Gaykema, W. P. J.; Volbeda, A.; Hol, W. G. J. *J. Mol. Biol.* **1986**, *187*, 255–275. (b) Volbeda, A.; Hol, W. G. J. *Proc. 4th Int. Symp. Oxid. Rel. Red. Sys.* **1988**, 291–307. (c) Volbeda, A.; Feiters, M. C.; Vincent, M. G.; Bouwman, E.; Dobson, B.; Kalk, K. H.; Reedijk, J.; Hol, W. G. J. Submitted for publication in *Eur. J. Biochem.* (d) Volbeda, A.; Hol, W. G. J. Manuscript in preparation.

(18) (a) Teo, B. K. In *EXAFS Spectroscopy: Techniques and Applications*; Teo, B. K., Joy, D. C., Eds.; Plenum: New York, 1981; pp 13–58. (b) Cramer, S. P.; Hodgson, K. O. *Prog. Inorg. Chem.* **1979**, *25*, 1–39. (c) Hasnain, S. S. *Life Chem. Rep.* **1987**, *4*, 273–331. (d) Hasnain, S. S.; Garner, C. D. *Prog. Biophys. Mol. Biol.* **1987**, *50*, 47–65.

(19) (a) Gurman, S. J.; Binsted, N.; Ross, I. *J. Phys. C* **1984**, *17*, 143–151. (b) Gurman, S. J.; Binsted, N.; Ross, I. *J. Phys. C* **1986**, 1845–1861.

(20) (a) Strange, R. W.; Blackburn, N. J.; Knowles, P. F.; Hasnain, S. S. *J. Am. Chem. Soc.* **1987**, *109*, 7157–7162. (b) Blackburn, N. J.; Strange, R. W.; McFadden, L. M.; Hasnain, S. S. *J. Am. Chem. Soc.* **1987**, *109*, 7162–7170.

(21) (a) Greaves, G. N.; Durham, P. J.; Diakun, G.; Quinn, P. *Nature* **1981**, *294*, 139–142. (b) Durham, P. J.; Pendry, J. B.; Hodges, C. H. *Solid State Commun. 38*, 159–162.

(22) Smith, T. A.; Penner-Hahn, J. E.; Berding, M. A.; Doniach, S.; Hodgson, K. O. *J. Am. Chem. Soc.* **1985**, *107*, 5945–5955.

(23) Kutzler, F. W.; Scott, R. A.; Berg, J. M.; Hodgson, K. O.; Doniach, S.; Cramer, S. P.; Chang, C. H. *J. Am. Chem. Soc.* **1981**, *103*, 6083–6088.

(24) Bianconi, A.; Congiu-Castellano, A.; Durham, P. J.; Hasnain, S. S.; Phillips, S. *Nature* **1985**, *318*, 685–687.

(25) Scott, R. A.; Hahn, J. E.; Doniach, S.; Freeman, H. C.; Hodgson, K. O. *J. Am. Chem. Soc.* **1982**, *104*, 5364–5369.

(26) Kau, L. S.; Spira-Solomon, D. J.; Penner-Hahn, J. E.; Hodgson, K. O.; Solomon, E. I. *J. Am. Chem. Soc.* **1987**, *109*, 6433–6442.

and in deoxy-Hc. We are particularly interested in the investigation of ligand binding to the Cu(I) centers, and demonstrate the usefulness of edge spectroscopy in the detection and characterization of CO binding to DBH and deoxy-Hc. As an aid to the interpretation of the edge data for the protein systems, we have chosen to study the X-ray absorption edge profiles of a number of Cu(I) complexes of the ligand systems N*n*PY2 and XYL-O– (Charts I and II), the chemistry of which is both well developed[12,13,15,16] and relevant[3] to the chemistry of the proteins themselves (since many of these Cu(I) complexes bind O_2 reversibly). These model complexes span the common coordination geometries and stereochemistries available to Cu(I) within the same tridentate ligand system and have allowed valuable correlations to be drawn between the energies and intensities of absorption edge features and the detailed stereochemistry at Cu(I). These correlations have been used to predict a model for CO binding to deoxy-Hc.

Materials and Methods

All of the complexes depicted in Charts I and II were synthesized as described elsewhere.[12a,13a,27–29] Superoxide dismutase was isolated according to the method of McCord and Fridovich.[30] Reduction of the native enzyme was achieved by addition of a 2-fold molar excess (per copper) of sodium dithionite in 10 mM sodium borate buffer, pH 10. Bovine DBH was isolated and reconstituted to eight Cu atoms per tetramer as described by Blackburn et al.[9a,b] Reduction was achieved by addition of a 2-fold molar excess (per copper) of ascorbate in acetate buffer, pH 6.00. *Panulirus interruptus* deoxy-Hc was prepared as described by Gaykema et al.,[17c] in 0.1 M Tris-HCl buffer, pH 8.75. *Busycon canaliculatum* Hc was prepared by extracting the hemolymph, followed by centrifugation at 10000*g* to clarify the extract, dialysis against 0.10 M sodium carbonate buffer, pH 9.8, and final concentration to ca. 5 mM in total copper content. CO derivatives were prepared by passing a stream of pure CO over a concentrated solution of the anaerobically reduced enzymes followed by anaerobic transfer to the EXAFS measuring cells.

X-ray Crystallography and Reduction of Diffraction Data. A dichloromethane/diethyl ether solution of compound **3**-$(PF_6)_2$ under Ar at room temperature yielded clear yellow crystals of $[Cu_2(N3OR)](PF_6)_2{\cdot}CH_2Cl_2$ that were suitable for X-ray crystallographic analysis. An epoxy-covered crystal was mounted on a Nicolet R3m four-circle automated diffractometer with a Mo X-ray source equipped with a highly ordered graphite monochromator ($\lambda(\text{Mo K}\alpha) = 0.71073$ Å). Automated centering and least-squares routines were carried out on 25 reflections for compound **3**-$(PF_6)_2{\cdot}CH_2Cl_2$ to obtain the cell dimensions that are given in Table I. A coupled θ(crystal) to 2θ(counter) scan mode was employed. The scan length was $(2\theta(K\alpha_1 - 1.0))$ to $(2\theta(K\alpha_2 + 1.0))^\circ$. Three check reflections were measured every 197 reflections; these exhibited no significant decay during data collection. The program XTAPE of the SHELXTL package[31a] was used to process the data. A summary of cell parameters, data collection parameters, and refinement results is found in Table I.

Table I. Crystallographic Data, Reduction of Intensity Data, and Summary of Structure Solution and Refinement for $[Cu_2(N3OR)](PF_6)_2{\cdot}CH_2Cl_2$

temp, K	294
a, Å	12.430 (4)
b, Å	13.456 (3)
c, Å	15.497 (4)
α, deg	81.75 (2)
β, deg	83.43 (2)
γ, deg	79.68 (2)
V, Å^3	2513.18
F(000)	1211.78
Z	2
D_{calcd}, g/cm^3	1.58
space group	$P\bar{1}$
cryst dimens, mm	0.40 × 0.20 × 0.50
scan rate, deg/min	12.0–30.0
scan range, deg	2.0–45.0
bkgd measurement	stationary crystal, stationary counter, at the beginning and end of each 2θ scan, each for the time taken for the scan
no. of reflcns measd	$+h,+k,+l$
no. of reflcns collcd	7108
no. of independent reflcns	3191, $\geq 6\sigma\lvert F_o\rvert$
abs coeff, cm^{-1}	11.04
data cor	bkgd, attenuators, and Lorentz and polarization effects in the usual fashion[a]
agreement between equiv reflcns	0.021
abs cor	not applied
atom scattering factors[b]	neutral atomic scattering factors used through the analysis
anomalous dispersion[c]	applied to all non-hydrogen atoms
R^d	0.0677
$R_w{}^d$	0.0701
goodness of fit[e]	1.742

[a] Hyde, J.; Venkatasubramanian, K.; Zubieta, J. *Inorg. Chem.* **1978**, *17*, 414. [b] Cromer, D. T.; Mann, J. B. *Acta Crystallogr., Sect. A* **1968**, *24*, 321. [c] International Tables for X-ray Crystallography; Kynoch Press: Birmingham, England, 1962; Vol. III. [d] $R = \sum[\lvert F_o\rvert - \lvert F_c\rvert / \sum\lvert F_o\rvert]$; $R_w = [\sum w(\lvert F_o\rvert - \lvert F_c\rvert)^2/\sum w\lvert F_o\rvert^2]^{1/2}$; $w = 1/\delta^2(F_o) + g(F_o)^2$; $g = 0.001$. [e] $\text{GOF} = [\sum w(\lvert F_o\rvert - \lvert F_c\rvert)^2/(\text{NO} - \text{NV})]^{1/2}$, where NO is the number of observations and NV is the number of variables.

Structure Solution and Refinement of Compound 3-$(PF_6)_2{\cdot}CH_2Cl_2$. The positional parameters of the copper atoms were determined by the Patterson method. The remaining non-hydrogen atoms were located by subsequent difference Fourier maps and least-squares refinements. Atomic scattering factors for neutral atoms were used throughout the analysis. Complex **3**-$(PF_6)_2$ crystallizes in the triclinic space group $P\bar{1}$ with $Z = 2$. Each asymmetric unit is found to contain one complete molecule. Anisotropic refinement was carried out on the copper atoms, oxygen atoms (O1 and O2),[31b] amine nitrogens (N1 and N4), chlorine atoms (solvent), and the atoms in the anion. The remaining atoms were refined isotropically. The hydrogen atoms were included in the final stages of refinement for the complex cation. Their isotropic thermal parameters were 1.2 times those of the carbons to which they were bonded. Carbon–hydrogen bond distances were fixed at 0.96 Å. One of the anions was found to be disordered. For this anion, eight fluorine atoms (F9–F16, which are attached to P atom P2), each with an occupancy factor of 0.5, were located beside two normal fluorine atoms (F7 and F8). When added together, they accounted for all the expected fluorine atoms in the molecule. A solvent of crystallization, identified as dichloromethane, was located in the final stages of refinement. The final *R* factors and refinement data are given in Table I. Structure factors, bond lengths, bond angles, anisotropic temperature factors, and hydrogen coordinates and temperature factors are available as supplementary material (Tables 4–8).

X-ray Absorption Measurements. X-ray absorption edges were measured on the Wiggler line 9.2 at the SRS, Daresbury Laboratory, by using an order-sorting Si(220) monochromator set to 50% harmonic rejection and with no focusing mirror installed. The spectra were calibrated in energy space by setting the maximum of the first feature on the absorption edge of copper metallic foil to 8982.0 eV, measured under identical conditions. The Cu(I) model compounds were loaded into thin aluminum sample cells anaerobically and measured in transmission mode as polycrystalline powders at ca. 70 K, under a reduced pressure of He. Protein samples were loaded into aluminum sample cells having rectangular apertures (12 × 3) fitted with 10-μm mylar windows, and their X-ray absorption edges were measured in fluorescence mode as frozen aqueous glasses (2–10 mM) at ca. 70 K or as a concentrated aqueous solution (*P. interruptus* deoxy-Hc) at ca. 293 K. The raw data were converted to energy space and normalized to the height of the smoothly varying background absorption determined by using standard background subtraction routines.[20] Values of absorption or fluorescence were taken

---

(27) Hendriks, H. M. J.; Birker, P. J. M. W. L.; van Rijn, J.; Verschoor, G. C.; Reedijk, J. J. *J. Am. Chem. Soc.* **1982**, *104*, 3607–3617.

(28) (a) Farooq, A. Ph.D. Dissertation, State University of New York at Albany, 1987. (b) Haka, M. S. Ph.D. Dissertation, State University of New York at Albany, 1987.

(29) (a) Karlin, K. D.; Hayes, J. C.; Hutchinson, J. P.; Hyde, J. R.; Zubieta, J. *Inorg. Chim. Acta* **1982**, *64*, L219. (b) Zubieta, J.; Karlin, K. D.; Hayes, J. C. *Copper Coordination Chemistry: Biochemical and Inorganic Perspectives* Karlin, K. D., Zubieta, J., Eds.; Adenine Press: Guiderland, NY, 1983; pp 97–108.

(30) McCord, J. M.; Fridovich, I. *J. Biol. Chem.* **1969**, *244*, 6049–6055.

(31) (a) All calculations were performed on a Data General Nova 3 computer with 32K of 16 bit words by using local versions of the Nicolet SHELXTL interactive crystallographic software package, as described in: G. M. Sheldrick, G. M. "Nicolet SHELXTL Operations Manual"; Nicolet XRD Corp.: Cupertino, CA, 1979. (b) Although oxygen atom O2 is refined anisotropically, in the ORTEP (Figure 1) isotropic displacement of this atom is shown for clarity.

Table II. Atom Coordinates ($\times10^4$) and Temperature Factors ($Å^2 \times 10^3$) for $[Cu_2(N3OR)](PF_6)_2{\cdot}CH_2Cl_2$[a]

atom	x	y	z	$U_{equiv/iso}$	atom	x	y	z	$U_{equiv/iso}$
Cu1	849 (1)	3919 (1)	1202 (1)	76 (1)*	C64	90 (9)	882 (8)	6567 (7)	80 (3)
Cu2	2557 (1)	1103 (1)	4513 (1)	61 (1)*	C65	856 (8)	1259 (7)	5931 (6)	56 (3)
O1	2499 (5)	3165 (4)	2874 (4)	55 (2)*	C66	1013 (7)	2342 (7)	5856 (6)	61 (3)
O2	1688 (6)	1844 (5)	2749 (5)	90 (3)*	C67	2188 (7)	2556 (7)	5728 (6)	59 (3)
N1	479 (6)	4740 (5)	2369 (5)	62 (3)*	C70	2414 (7)	2328 (7)	2524 (6)	52 (3)
N4	2641 (6)	2661 (5)	4770 (4)	54 (3)*	C71	3327 (7)	2105 (6)	1831 (5)	42 (2)
C1	1180 (8)	4648 (7)	3092 (7)	73 (3)	C72	3182 (7)	1491 (7)	1216 (6)	52 (3)
C2	1606 (7)	3580 (7)	3481 (6)	53 (3)	C73	4004 (7)	1309 (7)	542 (6)	54 (3)
C3	2064 (8)	3634 (7)	4337 (6)	71 (3)	C74	4956 (7)	1690 (6)	483 (5)	46 (2)
C5	5297 (11)	5436 (10)	3371 (9)	112 (4)	C75	5127 (8)	2249 (7)	1141 (6)	57 (3)
N2	−273 (7)	3125 (6)	1347 (5)	75 (3)	C76	4291 (7)	2455 (6)	1794 (6)	49 (2)
C21	−112 (10)	2213 (8)	1064 (7)	88 (4)	C81	5798 (7)	1557 (7)	−273 (6)	54 (3)
C22	−820 (11)	1510 (11)	1272 (8)	106 (4)	C82	5492 (9)	1832 (7)	−1120 (7)	70 (3)
C23	−1751 (11)	1814 (10)	1773 (8)	103 (4)	C83	6300 (9)	1795 (8)	−1849 (8)	86 (4)
C24	−1949 (10)	2694 (9)	2088 (8)	94 (4)	C84	7365 (10)	1451 (8)	−1681 (8)	88 (4)
C25	−1237 (9)	3382 (8)	1851 (7)	81 (3)	C85	7685 (10)	1152 (9)	−884 (8)	89 (4)
C26	−1396 (10)	4396 (10)	2153 (8)	107 (4)	C86	6906 (8)	1205 (7)	−158 (7)	71 (3)
C27	−629 (9)	4585 (10)	2761 (8)	98 (4)	F1	8465 (9)	7500 (6)	871 (5)	177 (6)*
N3	1970 (6)	4584 (6)	594 (5)	63 (2)	F2	9574 (6)	8223 (7)	1420 (6)	152 (5)*
C31	2650 (8)	4097 (8)	−16 (7)	71 (3)	F3	8490 (9)	9104 (7)	468 (6)	184 (5)*
C32	3522 (10)	4466 (9)	−486 (8)	95 (4)	F4	7088 (6)	8662 (9)	1328 (6)	187 (6)*
C33	3736 (11)	5405 (11)	−312 (9)	120 (5)	F5	8205 (8)	7753 (8)	2232 (5)	172 (5)*
C34	3068 (10)	5889 (10)	303 (8)	105 (4)	F6	8235 (8)	9386 (7)	1825 (7)	181 (5)*
C35	2191 (9)	5474 (8)	756 (7)	79 (3)	Cl1	6090 (3)	6328 (3)	2858 (2)	111 (2)*
C36	1474 (10)	6055 (9)	1450 (8)	105 (4)	Cl2	4805 (4)	4838 (4)	2604 (3)	167 (3)*
C37	459 (10)	5760 (9)	1872 (8)	97 (4)	P1	8345 (3)	8421 (2)	1361 (2)	72 (1)*
N5	3994 (6)	739 (5)	3909 (5)	55 (2)	P2	2460 (3)	6623 (3)	4885 (3)	99 (2)*
C51	4179 (8)	129 (7)	3261 (6)	66 (3)	F7	2429 (9)	6269 (8)	3986 (6)	190 (6)*
C52	5232 (8)	−108 (8)	2853 (7)	71 (3)	F8	2558 (10)	6976 (10)	5772 (6)	212 (7)*
C53	6058 (9)	247 (8)	3100 (7)	83 (3)	F9	1352 (15)	6109 (17)	5027 (13)	152 (10)*
C54	5903 (9)	882 (8)	3773 (7)	80 (3)	F10	2695 (14)	7706 (11)	4425 (11)	142 (8)*
C55	4828 (8)	1102 (7)	4159 (6)	60 (3)	F11	3820 (13)	6280 (16)	4914 (11)	137 (9)*
C56	4577 (8)	1734 (7)	4902 (7)	74 (3)	F12	3382 (18)	7164 (20)	4440 (20)	178 (15)*
C57	3821 (7)	2730 (7)	4717 (6)	63 (3)	F13	1298 (18)	7088 (22)	5209 (17)	154 (13)*
N6	1446 (6)	658 (5)	5363 (5)	53 (2)	F14	2303 (22)	5642 (15)	5482 (14)	140 (11)*
C61	1265 (8)	−319 (8)	5445 (7)	70 (3)	F15	3103 (23)	5564 (17)	5041 (19)	169 (14)*
C62	544 (8)	−730 (9)	6064 (7)	76 (3)	F16	1601 (22)	7599 (16)	4523 (19)	187 (15)*
C63	−36 (9)	−111 (9)	6621 (8)	89 (4)					

[a] Asterisks indicate values of equivalent isotropic U defined as one-third of the trace of the orthogonalized U_{11} tensor.

Table III. Selected Bond Distances and Angles for $[Cu_2(N3OR)](PF_6)_2{\cdot}CH_2Cl_2$

	Bond Distances (Å)		
Cu1–Cu2	6.262	Cu2–N4	2.212 (8)
Cu1–N1	2.214 (8)	Cu2–N5	1.935 (7)
Cu1–N2	1.878 (9)	Cu2–N6	1.912 (7)
Cu1–N3	1.881 (8)	O1–C2	1.455 (10)
	Bond Angles (deg)		
N1–Cu1–N2	102.0 (3)	N1–Cu1–N3	100.2 (3)
N2–Cu1–N3	156.6 (4)	N4–Cu2–N5	100.7 (3)
N4–Cu2–N6	104.9 (3)	N5–Cu2–N6	146.2 (3)

every 0.25 eV. Slits were adjusted so as to give maximum resolution, which was typically ±0.5 eV, as determined from visual inspection of the 8982.0-eV feature on the absorption edge of Cu foil. All the edges of the model complexes were measured on the same experimental station at the same spectral resolution. The copper foil calibration was checked before and after each set of edge measurements and was always found to be constant.

Results and Discussion

Description of the Structures of the Model Complexes. The model complexes used in the present study were chosen so as to span coordination geometries from linear two-coordinate to tetrahedral four-coordinate (Charts I and II). We first describe the structure of an important member of our series of model compounds, $[Cu_2(N3OR)](PF_6)_2{\cdot}CH_2Cl_2$ (**3**-$(PF_6)_2{\cdot}CH_2Cl_2$).

Description of the Structure of 3-$(PF_6)_2{\cdot}CH_2Cl_2$. The structure consists of one discrete complex dication and two well-separated anions per asymmetric unit. Final positional parameters are given in Table II. Selected bond distances and angles are given in Table III. An ORTEP view of the entire cation is shown in Figure 1, including the atom-labeling scheme.[31b] The two crystallographically independent cuprous ions are each three-coordinate with ligation from two pyridine and one tertiary amino donor groups.

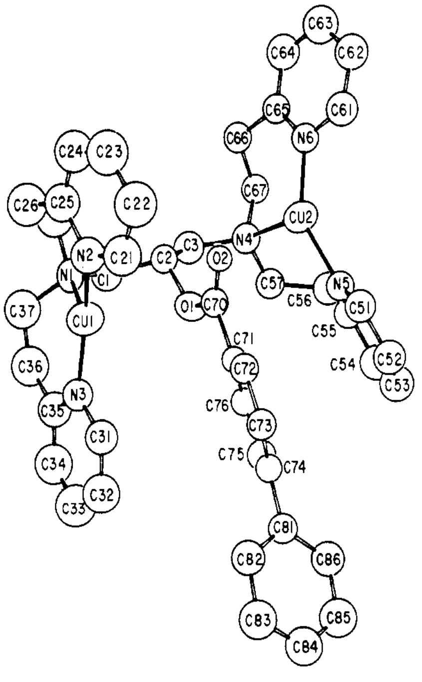

Figure 1. ORTEP diagram of the cationic portion of $[Cu_2(N3OR)](PF_6)_2]$ (**3**-$(PF_6)_2$), showing the atom-labeling scheme.

The bond distances found in the dication are in the range found for other three-coordinate Cu(I) complexes with N donors,[12a,15a] but the Cu–pyridine distances are among the shortest observed within the tripodal tridentate PY2 systems studied. Thus, the average Cu–py bond length of 1.90 Å is comparable to those in two other Cu(I) three-coordinate structures of the PY2 tridentate group, viz. $[Cu_2(m\text{-XYL})]^{2+}$[15a] (Cu–py = 1.92 Å) and $[Cu(BPY2)]^{+}$[32] (Cu–py = 1.88 Å) but is shorter than that found in the pseudo-four-coordinate complex $[Cu_2(N4PY2)(ClO_4)_2]$ (Cu–py = 1.94 Å), which has a coordinated perchlorate group at 2.55 Å.[13a] The Cu–N(amino) distances are long (2.21 Å) such that **3** may be thought of as a pseudo-two-coordinate complex dication. The consequence of this is that the three N atoms of the tridentate unit are only slightly distorted from planarity. The Cu(I) polyhedra extend away from one another (Cu1···Cu2 = 6.262 Å), with Cu1 lying 0.106 Å above the plane of N1, N2, and N3 and Cu2 lying 0.303 Å below the plane of N4, N5 and N6. The average out-of-plane distortion of the copper atoms is 0.205 Å. (This parameter will be important in the discussion of edge structure, and hereafter we denote the average out of plane distortion of the copper by the symbol *d*.) Considerable distortions from idealized trigonal-planar geometry are found since the *N*(amino)–Cu–py angles are acute (100–105°), resulting in a large py–Cu–py angle (Table III).

Structures of Other Model Compounds (Chart I). The dication $[Cu_2(EDTB)]^{2+}$ (**1**) contains linear two-coordinate Cu(I) centers coordinated to the imidazole N atoms of two benzimidazole groups;[27] $K[Cu(CN)_2]$ (K-**2**) in the solid state contains a chain of –Cu–C–N–Cu–C–N– atoms spiralling about a 2-fold screw axis. Each Cu is coordinated to two CN groups at 1.92 Å, with a longer bond to the N of the cyanide coordinated to the next copper atom in the chain. The Cu(I) centers are thus nearly trigonal-coplanar units with a distortion of the copper from planarity, *d*, = 0.22 Å.[33] $[Cu_2(N4PY2)(ClO_4)_2]$ (**4**-$(ClO_4)_2$) has a structure similar to that of **3** above, involving two pyridine groups at 1.944 and 1.934 Å and an amino N group at 2.145 Å coordinated to Cu(I), but with the important difference that the perchlorate counterion is weakly coordinated to the copper at 2.547 Å, such that the mean displacement of the Cu from the N_3 plane has increased to 0.417 Å, and the structure approximates a highly distorted tetrahedron with the perchlorate ion at the apex;[13a] a crystallographic 2-fold axis renders both Cu(I) centers equivalent. The monocation $[Cu^{I}(TEPA)]^{+}$ (**5**) is four coordinate, containing three pyridine groups at a distance of 1.99 Å (similar to that found in the tetrakis(pyridine)copper(I) monocation[34]) and a fourth weakly bound tertiary amino ligand at the longer distance of 2.20 Å.[29] The resulting structure is a flattened tetrahedron, with a displacement of Cu(I) from the N_3(pyridine) plane of 0.307 Å. Despite the formal description of **5** as a four-coordinate complex, the magnitude of the displacement *d* is in fact smaller than that found in complex **4**. $[Cu_2(N4PY2)(CH_3CN)]^{2+}$ (**6**), the acetonitrile adduct of **4**, is four-coordinate pseudotetrahedral;[13a] the acetonitrile ligand has displaced the perchlorate groups and now interacts strongly with the Cu(I) center as evidenced by a Cu–N(acetonitrile) distance of 1.945 Å and a long Cu–N(amino) distance of 2.151 Å. The copper atom thus exhibits a large displacement from the plane containing the three nitrogen atoms of 0.86 Å in the direction of the acetonitrile ligand.

Edge Studies on Cu(I) Model Complexes. Figure 2 shows the absorption and first-derivative edge data for complexes 1–6. The spectra of the complexes have low-energy features at 8983 (1), 8986 (1) (with the exception of **2**), and 8990 (1) eV in **1**, **4**, and **6**. The features at 8983 and 8986 eV have been assigned by Kau and co-workers[26] to transitions from the 1s core to $4p_z$ and $4p_{x,y}$ final states. (In our notation, the *z* axis is defined to be perpendicular to the N_3 plane (Figure 3); this is different from the notation of Kau and co-workers, where this direction is defined as the *x* axis.) However, it is clear from Figure 2 that the intensity of the 8983-eV peak varies in a systematic fashion and appears to correlate with the mean displacement *d* of Cu(I) from the N_3 plane. Thus, the amplitude of the peak is greatest for linear two-coordinate $[Cu(EDTB)]^{2+}$ (**1**, Figure 2a) and three-coordinate $[Cu(CN)_2]^-$ (**2**, Figure 2b) and decreases as the structure distorts through trigonal-pyramidal (**3**) toward pseudotetrahedral geometries (**4**–**6**). Thus, in complex **3**, which has only a small displacement of Cu(I) from the N_3 plane (d_{av} = 0.205 Å), the 8983-eV feature is present as a distinct peak whereas for **4**, in which the presence of the weakly coordinated perchlorate ion distorts the complex toward a pseudotetrahedral geometry (*d* = 0.417 Å), the peak diminishes to a shoulder and shifts to lower energy (Figure 2c,d). In four-coordinate $[CuTEPA]^+$ (**5**), the geometry is also flattened tetrahedral with only a small displacement of Cu(I) from the N_3(py) plane (*d* = 0.307 Å). Again, a well-resolved shoulder is observed on the absorption edge (Figure 2e). However, for the pseudotetrahedral complex **6**, (*d* = 0.856 Å), which is the acetonitrile adduct of **4** (Figure 2f), the 8983-eV peak disappears and new low-intensity shoulders are found at 8982 and 8985 eV, giving rise to a doublet pattern in the derivative spectra. The position of the lower energy peak appears to be the

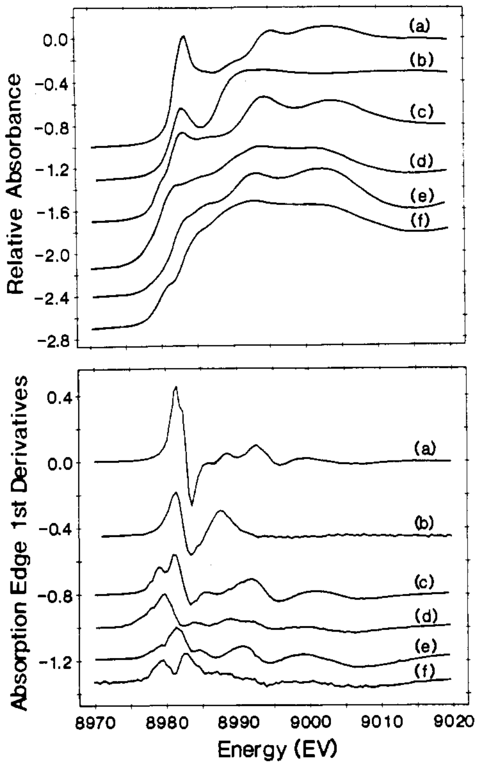

Figure 2. X-ray absorption K-edges and absorption edge first derivatives for the complexes depicted in Chart I. Spectra a–f refer to the spectra of complexes **1**–**6**, respectively.

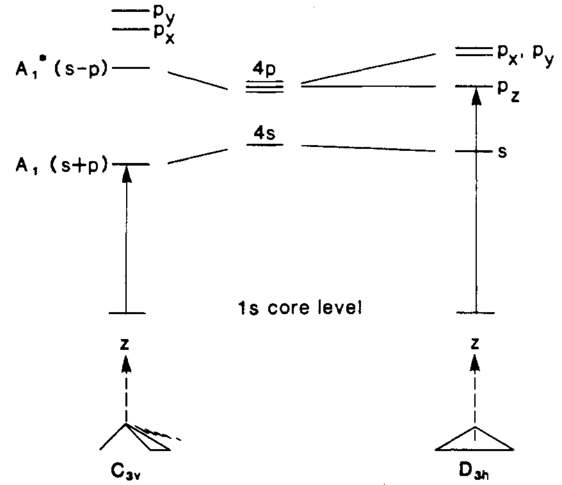

Figure 3. Qualitative ligand field diagram proposed to account for the intensities and relative energies of the major features of the absorption edges shown in Figure 2.

---

(32) Blackburn, N. J.; Karkin, K. D.; Concannon, M.; Hayes, J. C.; Gultneh, Y.; Zubieta, J. *J. Chem. Soc.* **1984**, 939–940.

(33) Cromer, D. T. *J. Phys. Chem.* **1957**, *61*, 1388–1392.

(34) Nilsson, K.; Oskarsson, A. *Acta Chem. Scand.* **1982**, *A36*, 605–610.

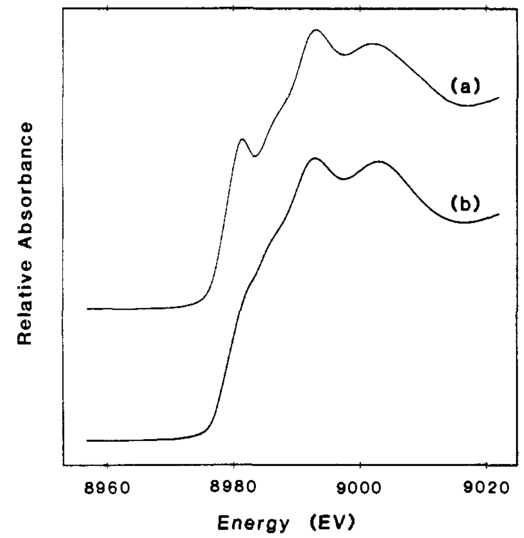

Figure 4. Absorption K-edges of (a) three-coordinate $[Cu_2(N3PY2)]^{2+}$ and (b) its four-coordinate carbonyl derivative, $[Cu_2(N3PY2)(CO)_2]^{2+}$.

end result of an additional trend in which a gradual shift of the 8983-eV peak to lower energy occurs as the structures distort toward tetrahedral, concomitant with the intensity decrease discussed above. In fact, close examination of the data in Figure 2 indicates that this trend is more advanced in complex **4** (d = 0.417 Å) than in complex **5** (d = 0.307 Å), which correlates with the increase in out-of-plane distortion, despite the fact that **5** has one more coordinated N-donor atom than **4**.

These trends can be rationalized in terms of the qualitative ligand field description given in Figure 3. The studies of Smith et al.,[22] and more recently Kau et al.,[26] have shown that the 8983-eV peak is almost certainly a $1s \rightarrow 4p_z$ transition. In either linear two-coordinate geometry or trigonal-planar (D_{3h}) geometry, the $4p_z$ final state is nonbonding and hence will be a pure p state localized on the metal. Mixing in of s character is forbidden by symmetry. The $1s \rightarrow 4p_z$ transition is thus strongly Laporte allowed and will be intense. However, as the geometry distorts toward trigonal pyramidal or pseudotetrahedral such that the copper atom domes out of the plane of the three nitrogen donor atoms, the symmetry is lowered to C_{3v} (or C_3) and the $4p_z$ and 4s orbitals then belong to the same (A_1) representation such that mixing of s character into the final state wave function can occur. The energy of the final (s + p) state should drop below that of the pure $4p_z$ orbital. Reduction in symmetry is thus expected to have the effect of decreasing the intensity of the 8983-eV band due to increasing Laporte forbidden character and of shifting the position to slightly lower energies. These predictions are entirely consistent with the data in Figure 2. The second peak observed at 8985 eV in the pseudotetrahedral complexes **4**–**6** could represent the $1s \rightarrow A_1^*$ transition (Figure 3), although other interpretations involving $4p_x$ and $4p_y$ combinations are equally probable as discussed by Kau et al.[26] We should also note that the effects of multiple scattering and increased covalency of the complexes can complicate the interpretation of absorption edge features such that any assignments must be tentative. This comment is particularly pertinent to those complexes having coordinated linear diatomic or triatomic ligands such as **2** and **6**, where multiple scattering resonances are expected to contribute strongly in the low-energy region. Nevertheless, the qualitative ligand field description given here is consistent with experimental observations and provides a basis for the interpretation of edge data for unknown systems.

Figure 4 shows edge data for the dinuclear Cu(I) complex of the ligand system N3PY2 (analogous to **4** but with a connectivity of three carbons rather than four between the amine N atoms) and its derivative with CO.[3b] Although the crystal structure of the parent complex $[Cu_2(N3PY2)](ClO_4)_2$ has not been reported, the structure of its CO derivative is known[3b,28b] and consists of discrete four-coordinate Cu(I) centers with an average displacement of the copper centers of 0.93 Å below the plane of the three N ligand atoms. The well-resolved, intense peak at 8982 eV (Figure 4a) is consistent with formulation of the parent complex as three-coordinate with only a small displacement of Cu(I) from the N_3 plane and suggests that, unlike the analogous N4PY2 complex, the perchlorate ion does not coordinate. Consistent with our ligand field analysis, coordination of CO (Figure 4b) diminishes the intensity of the 8982-eV peak substantially.

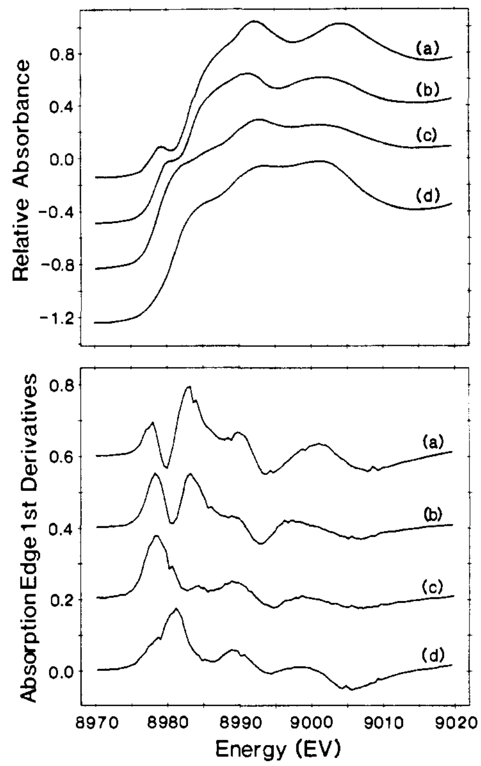

Figure 5. Absorption K-edges and absorption edge first derivatives for the complexes depicted in Scheme I: (a) complex **7**; (b) complex **9**; (c) complex **10**; (d) complex **8**.

Figure 5 shows absorption edge data for complexes of the ligand systems (XYL–O–) and (XYL–OH) (Chart II). The structure of **7** has been reported and consists of a pseudotetrahedral disposition of ligands around Cu(I), with one phenolate oxygen, one P from triphenylphosphine, one pyridine, and one amino N atom coordinated.[12a] Complexes **8**–**10** (which have not been characterized by crystallography) are derived from the same ligand system but with the bridging phenol protonated. By analogy to the bis(triphenylphosphine) adduct, the structure of which is known,[12d] the carbonyl (**9**) and acetonitrile (**10**) adducts of **8** are expected to be pseudotetrahedral.

Application of our ligand field model to the edge data shown in Figure 5 predicts structures generally consistent with the above arguments. Complex **8** exhibits a poorly resolved band of medium intensity at 8983–8985 eV (Figure 5d), which shifts to lower energy on coordination of acetonitrile (Figure 5c). The absorption edge of **8** (and its first derivative) is extremely similar in both intensity and position to that of complex **4** (compare Figures 5d and 2d), which implies distorted tetrahedral rather than three-coordinate geometry. By analogy to **4**, this may arise from interaction of a weakly coordinated perchlorate counterion with the Cu(I) centers or, alternatively, from a weak interaction of the phenolic OH group with one or both Cu(I) centers. Evidence in support of the latter structure comes from the absence of an O–H stretch in the IR spectrum of **8**, as compared to a well-defined ν(OH) in the IR spectra of **7** and **9**.[12d] (The presence of PPh_3 or CO as the fourth ligand is expected to abolish any tendency for coordination of the phenolic OH group.) For both the (pseudotetrahedral) triphenylphosphine (**7**, Figure 5a) and carbonyl complexes (**9**, Figure 5b) the band has decreased in energy to 8979 and 8980 eV, respectively. This pattern is similar to that found for complex **6**, $[Cu_2(N4PY2)(CH_3CN)_2]^{2+}$, and may reflect the increased covalency inherent in these complexes, due to both

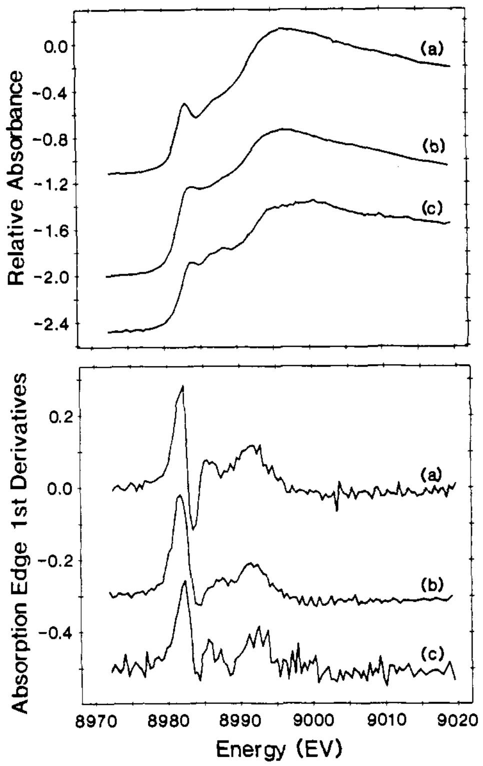

Figure 6. Absorption K-edges and first derivatives of (a) bovine Cu/Zn superoxide dismutase reduced with 2 equiv (per copper) of sodium dithionite, [Cu] = 2 mM; (b) bovine dopamine β-hydroxylase reduced with 2 equiv (per copper) of sodium ascorbate, [Cu] = 2 mM; (c) *P. interruptus* deoxyhemocyanin.

stronger σ-donor and π-acceptor interactions between Cu(I) and the PPh_3, CH_3CN, and CO ligands.[35]

Edge Studies on Cu(I) Derivatives of Copper Proteins. Figure 6 shows edge data for the Cu(I) sites of bovine SOD, DBH, and *P. interruptus* deoxy-Hc. It is evident that all three proteins exhibit features at 8983 (1) eV of varying intensity. Edge spectra for SOD and DBH resemble more closely the edge spectra of complex **3**-$(PF_6)_2$, indicative of a three-coordinate site with a small distortion of copper from the ligand plane: the 8983-eV band of the deoxy-Hc has less intensity, suggestive of a greater degree of distortion toward pseudotetrahedral geometry. No features are present at energies below 8983 eV, but all three proteins exhibit bands at higher energies, 8987 eV for reduced SOD, 8988.5 eV for reduced DBH, and a doublet of bands at 8986.5 and 8988 eV for deoxy-Hc.

The structure of native (Cu(II)) Cu/Zn SOD is known in detail both from a highly refined crystal structure[36] and from a wealth of spectroscopic data.[37] The Cu(II) is coordinated to four histidines (44, 46, 61, and 118), one of which (61) forms an imidazolate bridge to the neighboring Zn(II) atom. In contrast, structural details of the reduced, Cu(I) form of the enzyme are sparse. Available spectroscopic information favors three-coordination on the basis of the results of both EXAFS[38] and NMR.[39]

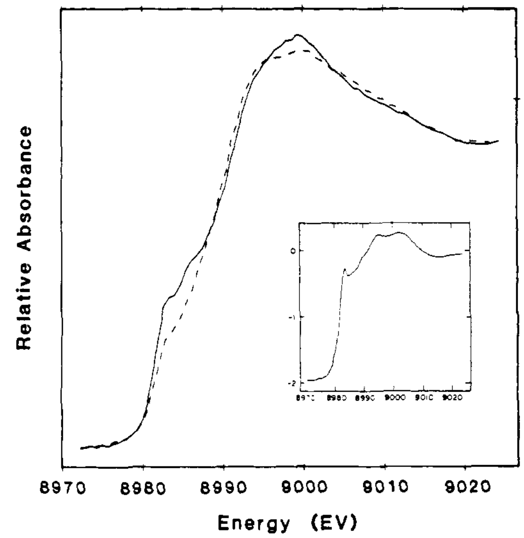

Figure 7. Comparison of K-absorption edges of *B. canaliculatum* deoxyhemocyanin (solid line) and its derivative with CO (dotted line). The inset shows a representation of a two- plus four-coordinate dicopper site, simulated by adding equal components of complexes **2** and **6** (Chart I).

The shortening of the Cu–N(imidazole) bond lengths (derived from EXAFS) from 1.99 Å in the oxidized form to 1.94 Å in the reduced form is consistent with a decrease in coordination number at copper. Furthermore, the 300-MHz ^1H NMR of the $Cu^I{}_2Co^{II}{}_2$ derivative of SOD clearly shows that the bridging his-61 ligand has dissociated from the Cu(I) center. The inference from the present work that the Cu(I) site of reduced SOD is three-coordinate with only minor distortions from planarity is thus fully supported by other data.

The Cu(I) sites of DBH also appear to be three-coordinate as judged by the 8983-eV feature. However, the 8983-eV peak is somewhat less well resolved and may suggest a more distorted site. Whereas continuous-wave-[9] and pulsed-EPR,[40] NMR relaxivity,[41] and EXAFS[42] studies on the native Cu(II) protein have implicated copper coordination to at least three histidine ligands, with additional ligation of one or two water molecules, the ascorbate-reduced Cu(I) derivative, which is believed to be the site of oxygen binding and activation,[5] appears from EXAFS studies to have quite different coordination involving two histidines and a sulfur ligand.[42b] Although two copper atoms are known to be involved in the benzylic hydroxylation of phenethylamines and related substrates by this enzyme, any structural inequivalence of the Cu^{2+} centers of the oxidized form has so far eluded detection by 9- or 35-GHz EPR[5,9a] or electron spin echo spectroscopy.[40] However, we have recently shown from potentiometric studies that the two coppers per subunit of DBH have binding constants for Cu^{2+} that differ by ca. 2 pK units at pH 5.[9a] Therefore, we must leave open the possibility that the 8983-eV feature may result from superposition of contributions from sites of differing coordination number or degree of distortion. One such possibility is two- plus four-coordination, as discussed below for Hc–CO and simulated in the inset to Figure 7.

The structure of the deoxy form of *P. interruptus* Hc is known from crystallography to involve a dinuclear Cu(I) site, each copper atom being coordinated to three histidine ligands.[17a–d] The presence of the dinuclear site[2,7,17a] limits interpretation of the edge data to the average coordination over both coppers. On the basis of the analysis of the data from the model compounds, the ab-

---

(35) Interaction of the filled d orbitals of the d^{10} Cu(I) with either empty π^* orbitals on CO or empty d orbitals on the P atom of PPh_3 could lead to a low-lying antibonding orbital that could act as the final state orbital of a $1s \rightarrow \pi^*$ type transition.

(36) (a) Tainer, J. A.; Getzoff, E. D.; Beem, K. M.; Richardson, J. S.; Richardson, D. C. *J. Mol. Biol.* **1982**, *160*, 181–217. (b) Tainer, J. A.; Getzoff, E. D.; Richardson, J. S.; Richardson, D. C. *Nature* (*London*) **1983**, *306*, 284–287.

(37) (a) Valentine, J. S.; Pantoliano, M. W. In *Copper Proteins*; Spiro, T. G., Ed.; Wiley: New York, 1981; pp 291–358. (b) Fee, J. A. In *Metal Ions in Biological Systems*; Sigel, H., Ed.; Marcel Dekker: New York, 1981; Vol. 13, pp 259–298. (c) Blackburn, N. J.; Strange, R. W.; McFadden, L. M.; Hasnain, S. S. *J. Am. Chem. Soc.* **1987**, *109*, 7162–7170.

(38) Blackburn, N. J.; Hasnain, S. S.; Binsted, N.; Diakun, G. P.; Garner, C. D.; Knowles, P. F. *Biochem. J.* **1984**, *219*, 985–990.

(39) Bertini, I.; Luchinat, C.; Monnanni, R. *J. Am. Chem. Soc.* **1985**, *107*, 2178–2179.

(40) McCracken, J. M.; Desai, P. R.; Papadoupolos, N. J.; Villafranca, J. J.; Peisach, J. J. *Biochemistry* **1988**, *27*, 4133–4137.

(41) Obata, A.; Tanaka, K. Kawazura, H. *Biochemistry* **1987**, *26*, 4962–4968.

(42) (a) Hasnain, S. S.; Diakun, G. P.; Knowles, P. F.; Binsted, N.; Garner, C. D.; Blackburn, N. J. *Biochem. J.* **1984**, *221*, 545–548. (b) Scott, R. A.; Sullivan, R. J.; DeWolfe, W. E.; Dolle, R. E.; Kruse, L. I. *Biochemistry* **1988**, *27*, 5411–5417.

sorption edge data on deoxy-Hc shown in Figure 6c would suggest considerable distortion from idealized trigonal geometry. Increased distortion is in fact consistent with the structural details emerging from the refinement of the crystal structure,[17d] which show that each copper atom is significantly distorted from the plane of its three histidine ligands and has at least one out of the three histidine ligands at a long distance (>2.4 Å). No protein-derived bridging ligand has been detected by crystallography, although a solvent-derived hydroxo or oxo bridge has not yet been ruled out.[17b] When compared with the data for the model compounds, the 8983-eV peak on the absorption edge of deoxy-Hc appears to be less intense than those of complexes with two short and one long Cu–N bond such as complex **3**-$(PF_6)_2$ (Figure 2) and is entirely consistent with a structure in which each Cu(I) ion is significantly displaced from the N_3 plane. The question of whether this distortion is imposed by conformational constraints of the histidine ligands, or by the presence of an additional (bridging) ligand, cannot be addressed by the absorption edge spectroscopy, but our data do suggest, as one possibility, the presence of an additional ligand, most likely a bridging hydroxo or oxo group, which may remain undetected at the 3.2-Å resolution of the crystal structure.

Carbonyl Derivatives. It is clearly difficult to be definitive about the structures of the Cu(I) centers in the native proteins on the basis of their individual absorption edge profiles. However, changes induced in the absorption edge spectra of a metal center upon binding of a ligand such as CO are more informative. Figure 7 shows a comparison of the absorption edges of *B. canaliculatum* Hc and its CO derivative. It is known that only a single CO binds to the dinuclear unit,[43] with an infrared stretching frequency (2063 cm^{-1}) in the range expected for terminally coordinated CO,[43,44] and it is generally accepted that CO binds to only one of the coppers of the dinuclear site.[45] Models for the structure of carbonmonoxy-Hc proposed previously, have involved 4 + 2 coordination, in which CO binds at one copper center to form a four-coordinate species (three N(his), one CO), leaving the second copper center coordinated to only two histidine ligands.[45,46] The rationale behind this structural model was the observation[46,47] that CO does not bind to two-coordinate Cu(I) complexes, which would then explain the 1:2 stoichiometry of CO to Cu(I) in Hc. Reed[45] has extended this model to include the possibility that a third histidine ligand may be weakly associated with the proposed two-coordinate center to give a T-shaped pseudo-two-coordinate species, which is more consistent with the presence of three histidines per copper, as suggested by the crystallography of the deoxy protein.

The edge studies on *B. canaliculatum* carbonmonoxy-Hc provide additional insight into these points. Since the edge features of the individual copper centers are additive, the proposed two-coordinate Cu(I) fragment of the dinuclear site should contribute an intense 8983-eV feature as 50% of the overall absorption (cf. compound **1**-$(ClO_4)_2$ (Figure 2) and edge features of complexes described in ref 26). Figure 7 includes, as an inset, a representation of the absorption edge of a two- plus four-coordinate dicopper species simulated by adding equal components of complexes **1** and **6**. The simulated spectrum retains a strong edge feature at 8983 eV, which is essentially absent in the absorption edge of Hc–CO. These considerations argue against the presence of a two-coordinate Cu(I) site in Hc–CO. Rather, the data indicate that CO binding produces changes that appear more consistent with conversion to a species whose geometry is close to tetrahedral at each copper. Additionally, the premise that the second copper must be two-coordinate because of its lack of reactivity toward CO has recently become less secure owing to the preparation of trigonal Cu(I)–N_2CO complexes of tropocoronand macrocycles[48] and CO adducts of two-coordinate Cu(I)–bis(imine) complexes.[49] A new interpretation, consistent with the present data, is the displacement of a bridging hydroxyl ligand by CO on one Cu center of deoxy-Hc, leaving two unbridged four-coordinated Cu(I) centers.

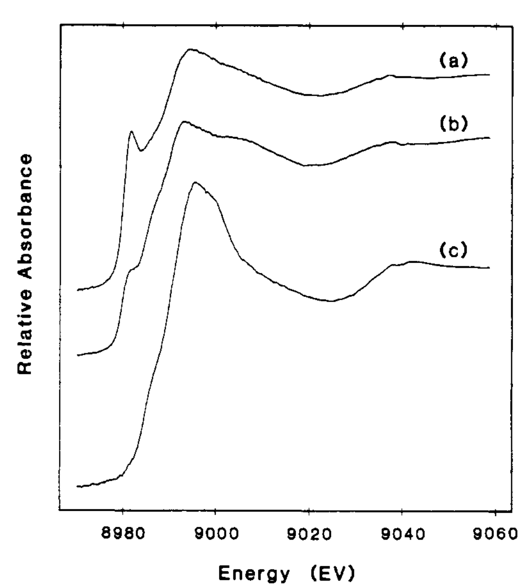

Figure 8. Comparison of K-absorption edges of dopamine β-hydroxylase and its derivative with CO: (a) ascorbate-reduced DBH; (b) ascorbate-reduced DBH incubated with 1 atm of CO; (c) native Cu(II) enzyme shown for comparison.

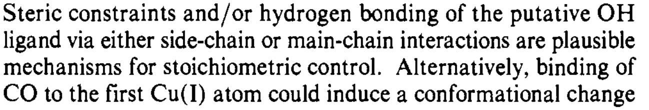

However, the absorption edge technique probably cannot distinguish between this and the alternative interpretation involving increased coordination at only one copper center via CO binding to give a three- plus four-coordinate active site.

The inaccessibility of the second Cu atom to CO binding remains an important question as regards both of these models. Steric constraints and/or hydrogen bonding of the putative OH ligand via either side-chain or main-chain interactions are plausible mechanisms for stoichiometric control. Alternatively, binding of CO to the first Cu(I) atom could induce a conformational change so as to block solvent/ligand access to the second Cu(I), as has been proposed by Sorrell and Borovick to explain the lack of solvent-mediated quenching of Hc–CO fluorescence.[50] We also note that CO binding to arthropodal Hcs is much weaker than binding to the molluscan proteins[43a] and gives rise to IR stretching frequencies 20 cm^{-1} lower than those of the molluscan analogues.[43b] These data emphasize the sensitivity of CO binding to perturbations in the environment of the copper centers.

Figure 8 shows the changes induced in the absorption edge spectrum of DBH upon binding of CO. It is clear that significant changes take place demonstrating that CO binds to the Cu(I) centers of the enzyme. The decrease in amplitude at 8983 eV is strong evidence for formation of a carbonyl adduct. However, the peak is not eliminated. Thus, we should consider the possibility that CO binds at only one of the two Cu(I) centers of the DBH monomeric subunit. We are actively pursuing the chemistry of the DBH–CO derivative to clarify this and other features of this interesting new derivative.

---

(43) (a) Fager, L. Y.; Alben, J. O. *Biochemistry* **1972**, *11*, 4786–4792. (b) Bonaventura, C.; Sullivan, B.; Bonaventura, J.; Bourne, S. *Biochemistry* **1974**, *13*, 4784–4789. (c) Munakata, M.; Kitagawa, S.; Goto, K. *J. Inorg. Biochem.* **1982**, *16*, 319–322. (d) Zolla, L.; Brunori, M. *Anal. Biochem.* **1983**, *133*, 465–469.

(44) Van der Deen, H.; Hoving, H. *Biophys. Chem.* **1979**, *9*, 169–179.

(45) Sorrell, T. N.; Jameson, D. L. *J. Am. Chem. Soc.* **1982**, *104*, 2053–2054.

(46) Reed, C. A. In *Copper Coordination Chemistry: Biochemical and Inorganic Perspectives*; Karlin, K. D., Zubieta, J., Eds.; Adenine: Guilderland, NY, 1983; pp 61–73.

(47) Pascali, M.; Floriani, C. In *Copper Coordination Chemistry: Biochemical and Inorganic Perspectives*; Karlin, K. D., Zubieta, J., Eds.; Adenine: Guiderland, NY, 1983; pp 311–330.

(48) Villacorta, G. M.; Lippard, S. J. *Inorg. Chem.* **1987**, *26*, 3672–3676.

(49) Casella, L.; Gullotti, M.; Pallanza, G.; Rigoni, L. *J. Am. Chem. Soc.* **1988**, *110*, 4221–4227.

(50) Sorrell, T. N.; Borovick, A. S. *Inorg. Chem.* **1987**, *26*, 1957–1964.

Conclusions

The prominent 8983-eV feature present on the absorption edge of Cu(I) complexes is sensitive not only to overall coordination number (as documented previously by Kau and co-workers[26]) but also to the details of the symmetry of the complex. Thus, in all the complexes studied a correlation was found between the intensity of this feature and the degree of distortion of the complex from two- or three-coordinate planar geometry toward tetrahedral.

These correlations have been applied to predict the geometry of the Cu(I) sites of SOD, DBH, and deoxy-Hc. Assignment of Cu(I)–SOD as a planar (or closely planar) three-coordinate center is possible. In the latter two cases the presence of more than one structural type of Cu(I) complicates the analysis, but comparison of the edge profile of deoxy-Hc with those of the model systems suggests distorted three- or four-coordination and hence the possible presence of an endogenous hydroxyl bridge.

The technique is particularly valuable in the study of ligand binding to Cu(I) centers in proteins. Here, comparative changes in absorption edge features allow ligand binding to be detected and any consequent changes in coordination geometry to be predicted. Using the latter approach, we have demonstrated the existence of a CO complex of DBH. In the case of *B. canaliculatum* deoxy-Hc, changes in the absorption edge upon CO binding to a single Cu atom[43] are consistent with trigonal-pyramidal or pseudotetrahedral geometry at each copper center of the dinuclear unit. The data indicate that each Cu center in Hc–CO is three- or four-coordinate and argue against previous proposals of two- plus four-coordination in Hc–CO.

Acknowledgment. We thank the Daresbury Laboratory for provision of beam time, computational facilities, and other necessary equipment for this study. Financial support is gratefully acknowledged from the SERC to N.J.B., NIH to K.D.K., and ZWO to J.R. We also thank the NATO Scientific Affairs Bureau for the award of a travel grant (RG.82/0139) to N.J.B. and K.D.K.

Supplementary Material Available: Listings of bond lengths, bond angles, anisotropic temperature factors, and hydrogen coordinates and temperature factors for complex **3**-$(PF_6)_2 \cdot CH_2Cl_2$ (Tables 4–7) (10 pages); listings of observed and calculated structure factors for **3**-$(PF_6)_2 \cdot CH_2Cl_2$ (Table 8) (38 pages).

Contribution from the Department of Chemistry, University of Georgia, Athens, Georgia 30602,
and Department of Physics, Emory University, Atlanta, Georgia 30322

Observation of $S = 2$ EPR Signals from Ferrous Iron–Thiolate Complexes. Relevance to Rubredoxin-Type Sites in Proteins

Mark T. Werth,[†] Donald M. Kurtz, Jr.,[*,†] Barry D. Howes,[‡] and Boi Hanh Huynh[‡]

Received September 15, 1988

In frozen solution the pseudotetrahedral ferrous iron–thiolate complexes with 2-mercaptoethanol, dithiothreitol, and glutathione (γ-glutamylcysteinylglycine) exhibit a low-field ($g \sim 10$) EPR signal below 30 K. This signal is ascribed to a transition within the $|\pm 2\rangle$ doublet of the $S = 2$ spin state, and these complexes appear to be the first examples of pseudotetrahedral ferrous complexes that give rise to such a signal. A detailed study was undertaken to ascertain the origin of this signal in the case of the complex with 2-mercaptoethanol. $Ba[Fe(SCH_2CH_2OH)_4]$ was prepared and shown to contain an FeS_4 site of approximate tetrahedral symmetry by X-ray crystallography. For $[Fe(SCH_2CH_2OH)_4]^{2-}$ in water, the 1–/2– midpoint reduction potential (–0.35 V vs SCE) and ^1H NMR (δ(Fe–SCH_2CH$_2$OH) 203 ppm at 25 °C) and ^{57}Fe Mössbauer ($\Delta E_Q = 3.48 \pm 0.03$ mm/s, $\delta = 0.73 \pm 0.02$ mm/s at 4.2 K) spectra show that this complex, and essentially only this complex, survives in solution, when the mole ratio of thiolate to iron is 4 or greater. Mössbauer spectra obtained in applied fields up to 7 T reveal at least two species in frozen aqueous solutions of $[Fe(SCH_2CH_2OH)_4]^{2-}$. Spectral simulations show that the major (75%) and minor (25%) species have spin Hamiltonian parameters strongly resembling those of reduced rubredoxin and reduced desulforedoxin, respectively. The minor species has values of zero-field splitting parameters ($D = -5.0 \pm 2.0$ cm^{-1}, $E/D = 0.17 \pm 0.05$) that are consistent with observation of an $S = 2$ EPR signal at low field. The slightly larger values of these parameters for reduced desulforedoxin preclude the observation of an $S = 2$ EPR signal from this protein. The two species of $[Fe(SCH_2CH_2OH)_4]^{2-}$ in solution are ascribed to different sets of S–Fe–S angles. Since variations in these angles are expected to have relatively low energy barriers, observation of an $S = 2$ EPR signal from biological Fe(Cys-*S*)$_4$ sites is likely to be strongly dependent on the protein matrix.

As part of a search for new spectroscopic probes of high-spin ferrous centers in proteins, we have examined the simplest such prototype for iron–sulfur proteins, namely, the pseudotetrahedral Fe(Cys-*S*)$_4$ site in reduced rubredoxin (Cys-*S* = cysteine thiolate). We have recently added ^1H NMR to the list of spectroscopies that can elicit characteristic signals from the ferrous Fe(Cys-*S*)$_4$ site in rubredoxin.[1] Judging from a number of recent reports,[2–5] EPR signals arising from integer spin states represent an increasingly important electronic probe of iron sites in proteins. We now report that the $S = 2$ state of ferrous $Fe(SR)_4$ complexes can exhibit a characteristic EPR signal. We also delineate some structural and spectroscopic parameters that favor observation of such a signal.

Experimental Section

All manipulations were carried out at room temperature under an Ar atmosphere in either Schlenk-type glassware or septum-capped vials attached to a vacuum manifold. Solutions were added and transferred via steel tubing or gastight syringes. The thiols used for this study, 2-mercaptoethanol, dithiothreitol, glutathione, and lipoic acid, were obtained commercially and used without further purification. D,L-Dihydrolipoate was prepared from the oxidized compound as previously described.[6] The following general procedure was used to prepare ferrous $Fe(SR)_4$ complexes in situ. The thiol was dissolved in the desired solvent (either water or DMSO) with sufficient LiOH to deprotonate thiol groups plus any carboxylate groups. Iron was then added as solid $FeCl_2$ or $Fe(SO_4) \cdot 7H_2O$. A thiolate/iron mol ratio ≥ 4 was maintained in all solutions. This procedure was previously shown to generate stable solutions of the ferrous $Fe(SR)_4$ complexes in water.[1] Specific reagent concentrations are given in the figure legends. Solutions for electrochemistry were ~4 mM in iron and ~100 mM in total thiol. These

---

[†] University of Georgia.
[‡] Emory University.

(1) Werth, M. T.; Kurtz, D. M., Jr.; Moura, I.; LeGall, J. *J. Am. Chem. Soc.* **1987**, *109*, 273–275.
(2) Hendrich, M. P.; Debrunner, P. G. *J. Magn. Reson.* **1988**, *78*, 133–141.
(3) Reem, R. C.; Solomon, E. I. *J. Am. Chem. Soc.* **1987**, *109*, 1216–1226.
(4) Hagen, W. R.; Dunham, W. R.; Johnson, M. K.; Fee, J. A. *Biochim. Biophys. Acta* **1985**, *828*, 369–374.
(5) Hagen, W. R. *Biochim. Biophys. Acta* **1982**, *708*, 82–98.
(6) Bonomi, F.; Werth, M. T.; Kurtz, D. M., Jr. *Inorg. Chem.* **1985**, *24*, 4331–4335.

0020-1669/89/1328-1357$01.50/0